

# A novel studies on electrical behaviour of chemically synthesized conducting polyindole

N S Wadatkar<sup>1\*</sup> and S A Waghuley<sup>2</sup>

<sup>1</sup>Department of Physics, Government Polytechnic, Yavatmal 445001, India

<sup>2</sup>Department of Physics, Sant Gadge Baba Amravati University, Amravati 444 602, India

Received: 04 December 2017 / Accepted: 08 May 2018 / Published online: 30 July 2018

**Abstract:** This research article is intended for the novel study of thermal, electrical and dielectric properties of conducting polyindole (PIn) as-synthesized through chemical oxidative route. The characterization techniques such as Fourier transform infrared spectroscopy; X-ray diffraction and Thermo gravimetric-differential thermal analysis ensured the structural and thermal properties of the as-synthesized materials. The dielectric measurements of the samples were performed through AC impedance analyser in the frequency and temperature ranges from 20 Hz–1 MHz to 308–393 K respectively. The variation of AC conductivity with frequency obeys Jonscher's universal power law. The modulus spectra depicted the non-Debye nature of the material. The dielectric studies of as-synthesized PIn samples validate their potential utilization for energy storage application. The thermal study ensures that, the synthesized samples have fairly good thermal stability.

**Keywords:** Chemical polymerisation; Polyindole; Electrical properties

**PACS Nos.:** 72.00.00; 72.80.-r; 72.80.Le

## 1. Introduction

In recent years, an aromatic nitrogenous conducting polymers have been studied intensively that could find an enormous amount of applications in different areas such as, rechargeable batteries [1], light emitting diodes [2], sensors [3, 4], electrochemical supercapacitors [5], memory storage devices [6] and electrochromic displays [7]. Polyindole (PIn) is one of the aromatic nitrogenous conducting polymers investigated in detail with several advantages in various electronics applications, due to its fairly good electrical conductivity, good redox activity and high stability as compared with other conducting polymers [8, 9]. PIn is a conducting electroactive polymer. The indole monomer can be normally polymerized after anodic oxidation in various electrolytes. The electrochemical oxidation of indole in LiClO<sub>4</sub> containing acetonitrile electrolyte solution gives electro-chromic polymer film received fairly good air stability and depending upon synthesis procedure,

type and nature of dopant ions, its conductivity ranges about  $10^{-3}$ – $10^{-1}$  S cm<sup>-1</sup> [10]. It has been rumoured within the literature that synthesis techniques and concentration of dopants, and some additives, like surfactants, introduced during synthesis have effects on polymerization yield and any other physical properties of PIn such as morphology, electrical conductivity, thermal and mechanical behaviour.

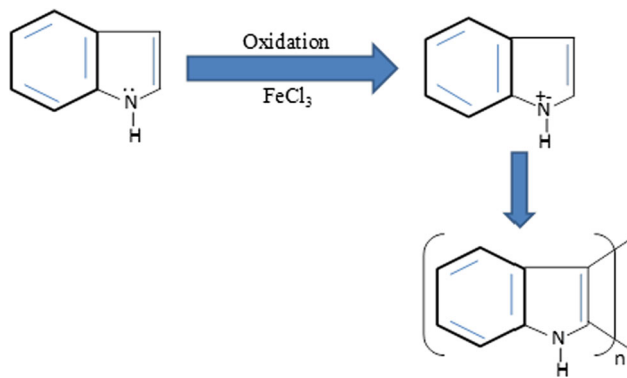
The conducting polymer, PIn, has been primarily synthesized by either chemical or electrochemical process [1, 11, 12]. Joshi et al. [13] have synthesized nanosized gold (Au) and PIn composite via in situ polymerization of indole, using metal salt chloro-auric acid as an oxidant, in a microemulsion system. Recently, chemical synthesis of conducting polymers has got much more importance not only because of requirement of bulk quantity of polymers but also due to the need of the particular morphology of conducting polymers. In the conventional chemical synthesis of conjugated conducting polymers are generally formed with granular morphology and amorphous nature [14–16]. Rajasudha et al. [17] reported that the synthesis of PIn by the chemical oxidation method using SDS as steric

\*Corresponding author, E-mail: nswadatkar81@gmail.com

stabilizer and obtained fine particles with 20 nm average particle size. Wadtkar et al. [18] have studied the complex optical properties of chemically synthesized PIn by using  $\text{FeCl}_3$  as an oxidant in aqueous solution.

In the present work, indole (In), the monomer of PIn, has been polymerized via chemically oxidative polymerization in the presence of an oxidant ( $\text{FeCl}_3$ ) in aqueous solution. There is no report on chemical synthesis of conducting PIn in universal solution till date. The present research article is an integrated report, which unified the thermal, electrical and dielectric properties with varying temperature of as-synthesized polymeric materials. The characterization techniques such as Fourier transform infrared spectroscopy (FTIR), X-ray diffraction (XRD) and Thermo gravimetric-differential thermal analysis (TG-DTA) were employed to study the structural and thermal properties of the derived materials.

The chemical oxidative polymerization method is frequently used for the synthesis of conducting polymeric materials from different classes of monomers like aniline, indole, pyrrole, etc. In this technique, the monomer is characterized by electron donor properties and high oxidation tendency due to presence of electron donor substituent in benzene or heterocyclic ring [19]. The oxidative polymerization of monomer is takes place due to the action of oxidizing agent. Generally, metal chloride is used as an oxidizing agent. The cation or cation radical sites are generated in monomer during this process, so formation of covalent bond between monomer molecules and monomer form the chain structure [20]. During the chemical polymerization, temperature of the process is generally raises. The majority of oxidative polymerization reactions are exothermic. Scheme 1 shows the mechanism involves in the chemical oxidative polymerization of PIn.



**Scheme 1** Mechanism of chemical polymerization of PIn

## 2. Experimental

Indole monomers, anhydrous iron (III) chloride ( $\text{FeCl}_3$ ), and hydrogen peroxide ( $\text{H}_2\text{O}_2$ ) from SD Fine Chemicals (AR-grade) were employed in the current study without further purification. The indole monomer was used as received for synthesis of PIn. The different samples of PIn were synthesized according to chemical oxidative polymerization method [18] by varying the stoichiometric ratios of indole and  $\text{FeCl}_3$  as 70:30, 60:40, 50:50, 40:60 and 30:70 wt%.

The samples were characterized through FTIR, XRD and TG-DTA techniques. The FTIR spectrum was recorded on Shimadzu (Model-8201) spectrophotometer. The FTIR was taken in the KBr medium at room temperature in the region  $4000\text{--}400\text{ cm}^{-1}$  at scan rate 16. The XRD pattern of powder sample was recorded on Rigaku miniflex-II X-ray diffraction using  $\text{CuK}_\alpha$  radiation ( $\lambda = 1.54\text{ \AA}$ ) in the  $2\theta$  range of  $10\text{--}70^\circ$ . The TG-DTA was carried out on Shimadzu DTG-60h thermal analyser under nitrogen flow at the heating rate of  $10\text{ }^\circ\text{C min}^{-1}$ . The temperature of the sample varied from room temperature to  $600\text{ }^\circ\text{C}$ . For electrical measurements, samples were polished and conducting silver paste was deposited on either sides. The sample area was taken to be the area exposed to the electrode surface. The two silver electrodes were used to sandwich the sample in four probe cell technique. The AC impedance measurements were performed through LCR meter, Agilent Technology, Singapore, interfaced to a computer for data acquisition over frequency range  $20\text{ Hz--}1\text{ MHz}$  and a temperature range  $303\text{--}393\text{ K}$ . The LCR meter was used in sandwich configuration in the present study.

## 3. Results and discussion

### 3.1. FTIR analysis

Figure 1 shows the FTIR spectra of PIn powder samples obtained from chemical oxidative polymerization with different stoichiometric ratio of indole and  $\text{FeCl}_3$  as (a) 70:30 (b) 60:40, (c) 50:50, (d) 40:60 and (e) 70:30 wt%. The strong peak at  $3496\text{ cm}^{-1}$  observed in the spectra represents the characteristics absorption of the N-H bond, which can be ascribed to stretching vibration [21, 22]. The band at  $1506\text{ cm}^{-1}$  can be ascribed to be the deformation vibration of the N-H bond [23]. This can be the inference that there are still N-H bonds on PIn backbone. The spectrum showed the peaks at  $1415$  and  $1690\text{ cm}^{-1}$  are due to stretching mode of aromatic alkene and the peak at  $725\text{ cm}^{-1}$  is due to bending mode of the aromatic alkene. The single peak located at  $1452\text{ cm}^{-1}$  is assigned to the

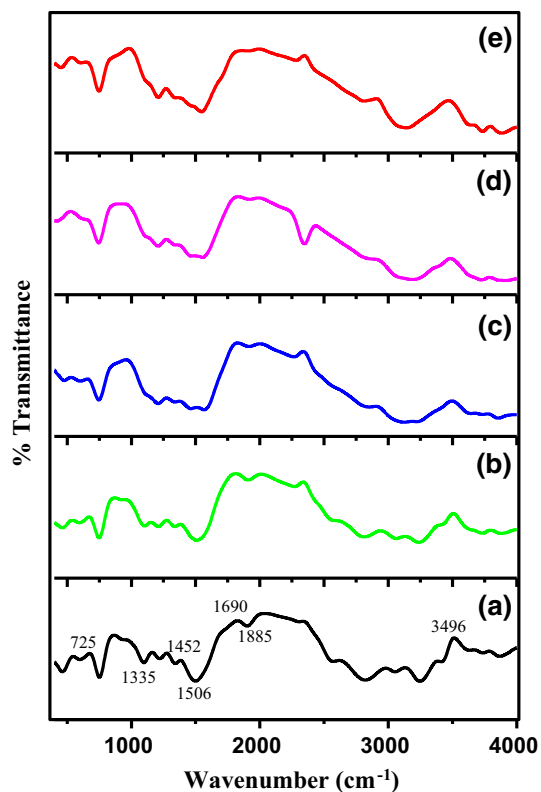


**Fig. 1** FTIR spectra of PIn samples for different stoichiometric ratios of indole and  $\text{FeCl}_3$  as (a) 70:30, (b) 60:40, (c) 50:50, (d) 40:60 and (e) 30:70 wt%

stretching mode of the benzene ring [24]. The band at  $1335\text{ cm}^{-1}$  is attributed to the modes involving the  $\text{C}_8\text{-N-C}_2\text{-C}_3$  group.

### 3.2. XRD analysis

Figure 2 depicts the XRD patterns of the samples of PIn with different stoichiometric ratio of indole and  $\text{FeCl}_3$  as (a) 70:30, (b) 60:40, (c) 50:50, (d) 40:60 and (e) 30:70 wt%. The broad humps are observed in the XRD profile, which attributes to amorphous nature of as-synthesized samples of PIn. In each case broad peaks are observed at about  $2\theta = 26.22^\circ$ ,  $26.25^\circ$ ,  $26.32^\circ$ ,  $26.42^\circ$  and  $26.40^\circ$ . The broad peaks are the characteristic of amorphous PIn [21] and are due to the scattering from PIn chains at the interplanar spacing. However, the position of the maximum intensity of the amorphous halos is different from each other for each sample. It may be interested to note that the peak position of these amorphous halos depends on the concentration of oxidant. The average chain separation can be calculated from these maxima using the relation [25].

$$R = 5\lambda/8 \sin \theta \quad (1)$$

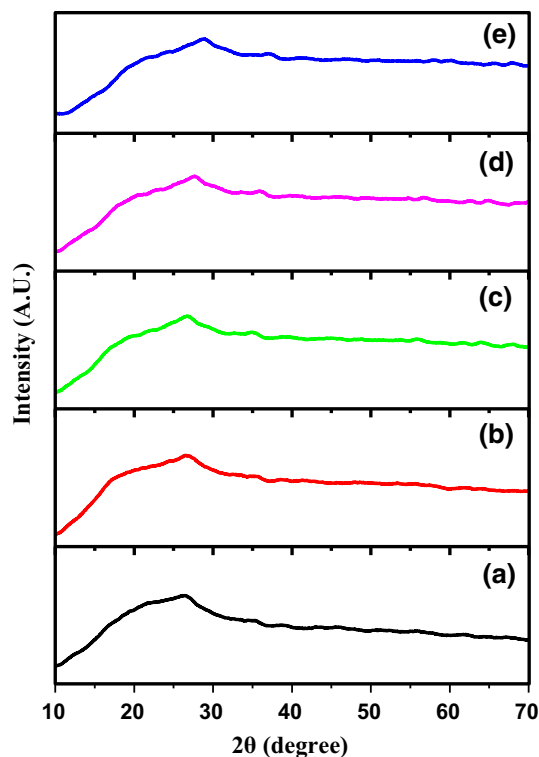


**Fig. 2** XRD pattern of PIn samples for different stoichiometric ratios of indole and  $\text{FeCl}_3$  as (a) 70:30, (b) 60:40, (c) 50:50, (d) 40:60 and (e) 30:70 wt%

where  $R$  is the polymer chain separation,  $\lambda$  is the X-ray wavelength and  $\theta$  is the diffraction angle at the maximum intensity of amorphous halos. The values of average polymer chain separation are listed in Table 1.

### 3.3. Thermal analysis

The thermal decomposition of polymers can be analysed by thermogravimetry technique. The typical TG curves of normalized weight and derivative thermogravimetry (DTG) data of the derivative weight of PIn with stoichiometric ratios (50:50, 40:60, and 30:70) wt% of indole and  $\text{FeCl}_3$  are plotted as a function of temperature and shown in Fig. 3a–c respectively.

The small weight loss of 3% observed in TG obtained in air could be due to a loss of moisture trapped in the polymer samples [26]. The dopant elimination occurs between 453 and 633 K with a weight loss of about 30%. The backbone rupture begins after the dopant elimination, which leads to a further weight loss of about 45% at 785 K [27].

**Table 1** Values of average polymer chain separation of as-synthesized PIn with different stoichiometric ratio of indole and FeCl<sub>3</sub>

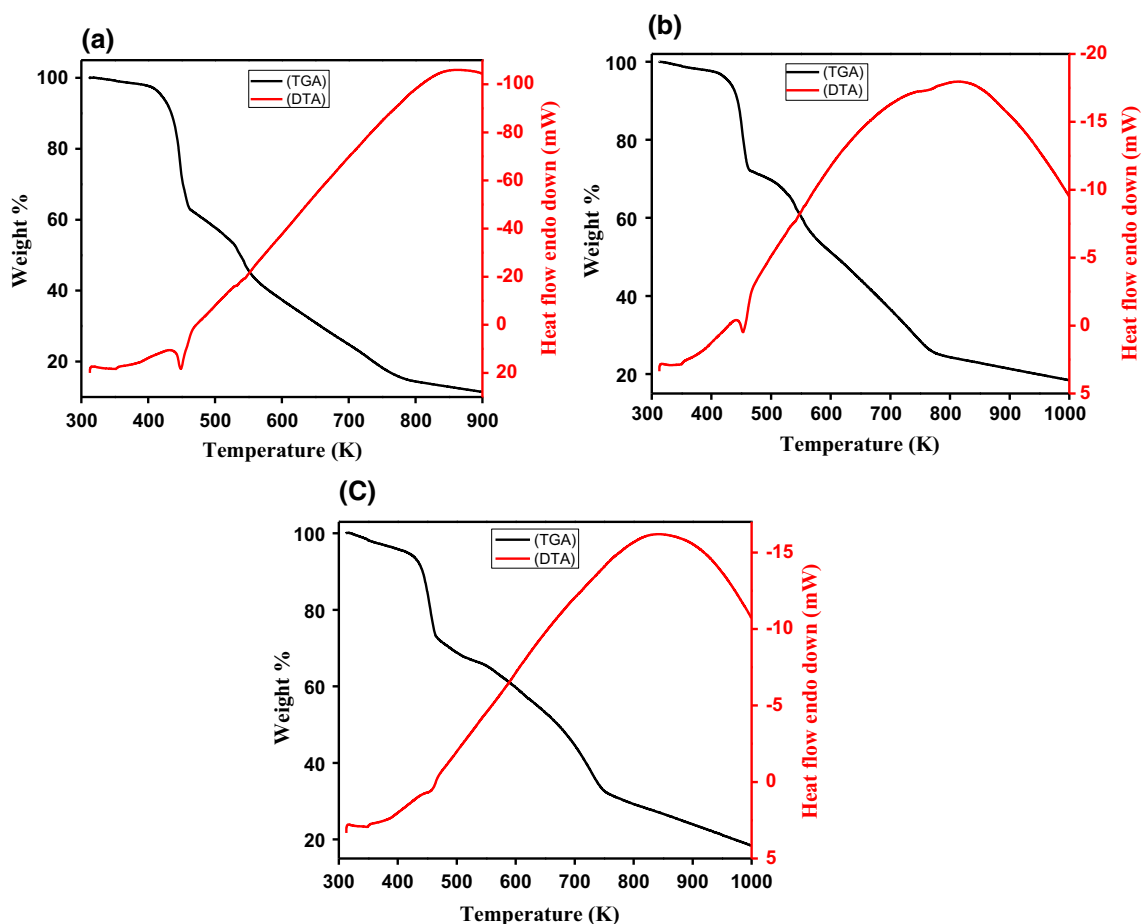
wt% ratios	Prominent peak position (2 $\theta$ )	Average polymer chain separation (Å)
70:30	26.22°	1.86
60:40	26.25°	1.81
50:50	26.32°	1.72
40:60	26.42°	1.60
30:70	26.40°	1.62

### 3.4. AC conductivity measurements

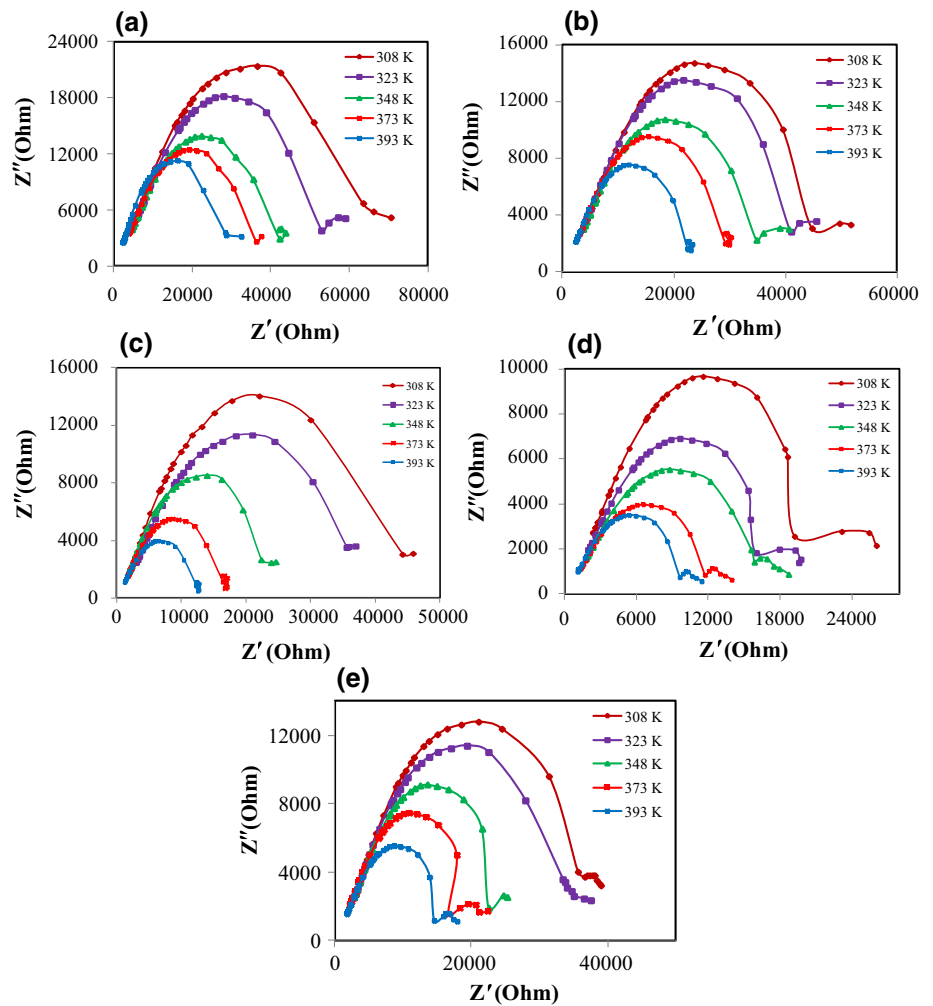
Complex impedance measurements were carried out to determine the electrical conductivity and also the AC behaviour of PIn over wide ranges of temperature and frequency. The temperature-dependent impedance data of all the samples of PIn are analyzed. Figure 4 shows the impedance plot ( $Z'$  versus  $Z''$ ) obtained for the samples PIn with different stoichiometric ratios of indole and FeCl<sub>3</sub> at different temperatures. The trend of impedance obtained is almost a semicircle exhibiting the single conduction mechanism [28]. The centre of each semicircle is found to

be depressed below the real axis. This referred that associated relaxation of charges (Polaron or free ions) represents non-Debye in nature [29]. The semicircle obtained is decreases gradually with the rise of temperature showing that the sample is more conductive at higher temperature. A depressed semicircle is obtained by the extrapolation of this plot. This depressed semicircle at the high frequency region arises from the bulk relaxation effects. In some cases, another semicircle is observed may be due to the dopant remains as an impurity in the sample.

The study of frequency dependent conductivity spectra could be well-established methodology for characterizing the hopping dynamics of ions. Figure 5(a–e) shows frequency-dependent conductivity plot of  $\log(\sigma)$  versus  $\log(\omega)$  for the PIn with stoichiometric ratios of indole and FeCl<sub>3</sub> as (70:30–30:70) wt% at various temperatures. The conductivity is found to be nearly frequency-independent within the low frequency region, suggesting that, the ionic diffusion is random less via activated hopping process. At high frequency region, dispersion in conductivity has been ascertained. The high frequency dispersion is predominant at lower temperatures. From Fig. 5, it is ascertained that

**Fig. 3** TG-DTA Plots of PIn powder samples for stoichiometric ratios of indole and FeCl<sub>3</sub> as (a) 50:50, (b) 40:60 and (c) 30:70 wt%

**Fig. 4** Cole-cole plot for as-synthesized samples of PIn with stoichiometric ratios of indole and FeCl<sub>3</sub> as (a) 70:30, (b) 60:40, (c) 50:50, (d) 40:60 and (e) 30:70 Wt %



the dispersion becomes prominent as shifted to higher frequency region with rise in temperature. The frequency dispersion characteristic within the high frequency region has been analysed using Jonscher's universal law relation [30, 31].

$$\sigma(\omega) = \sigma(0) + A\omega^n \quad (2)$$

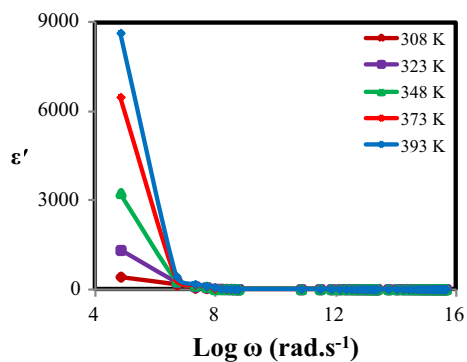
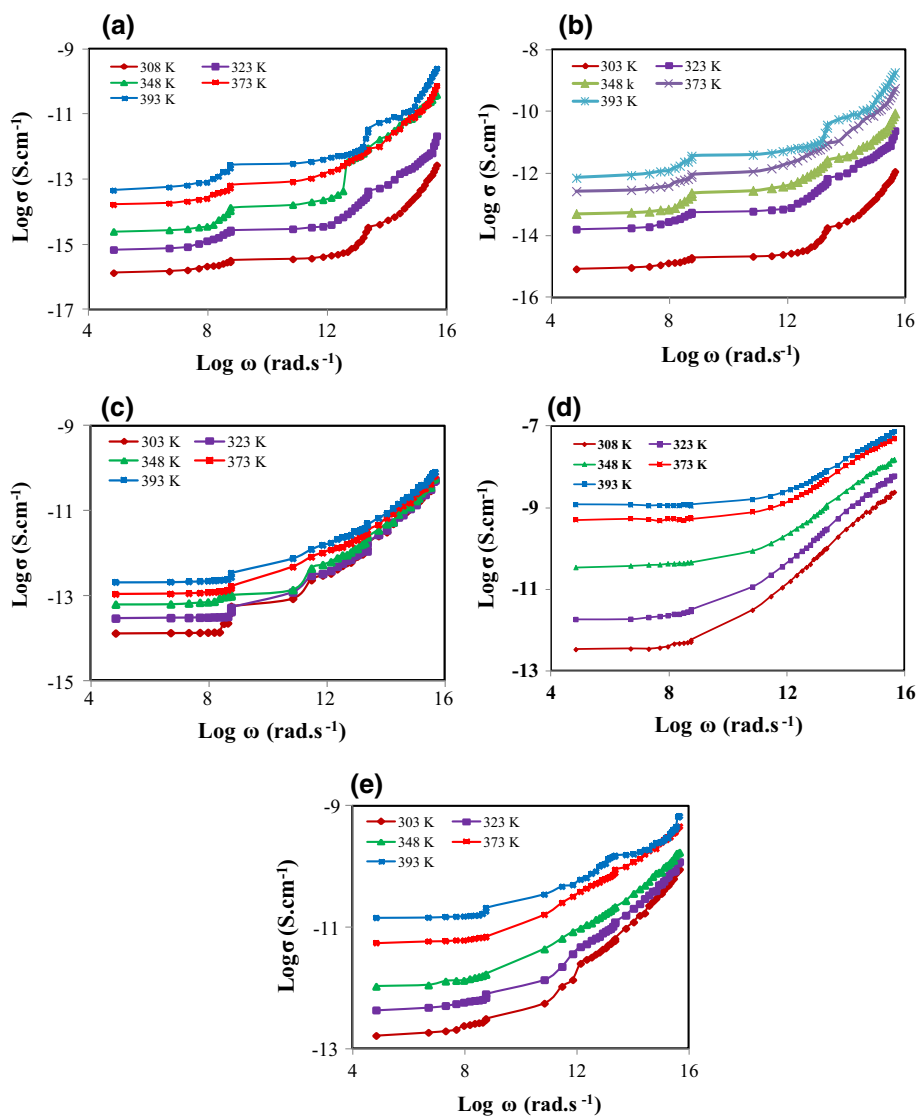
where  $\sigma(0)$  is the frequency-independent DC conductivity of the sample,  $A$  is a weakly temperature-dependent quantity and  $n$  is the power law exponent lying in the range  $0 < n < 1$ . The conductivity data of all PIn samples with different wt% of indole and FeCl<sub>3</sub> have been fitted to the above equation [Eq. (2)]. The fitted curves are represented by the solid lines in the Fig. 5 shows reasonably good agreements with the experimental ones.

Figure 6 shows the frequency dependence plots of the real part of dielectric constant ( $\epsilon'$ ) at various temperatures for PIn with (40:60) wt% of indole and FeCl<sub>3</sub>. It is found that the value of dielectric constant for the polymeric samples decreases with frequency at a particular temperature. This ensured that the concentration of charge carriers

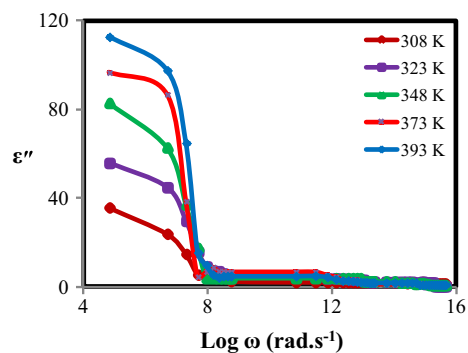
decreases with the frequency and attains a constant value which may be due to the effect of more rapid polarization process in the sample [32]. In all the cases, above  $10 \text{ rad s}^{-1}$  the permittivity is observed to be nearly frequency independent. However, a strong frequency dispersion of permittivity is observed in the low frequency region. The decrease of dielectric constant with frequency may be attributed to the electrical relaxation mechanism [33, 34]. It is found that the temperature dependence of dielectric relaxation peak  $\omega_m$  obeys a simple Arrhenius relation,  $\omega_m = \omega_{m0} \exp(E/KT)$  [35].

Figure 7 depicts the frequency dependence plots of imaginary part of dielectric constant ( $\epsilon''$ ) at various temperatures for PIn with (40:60) wt% of indole and FeCl<sub>3</sub>. In this figure it is observed that the loss factor  $\epsilon''$  exhibit the loss peak in the high frequency region. This behavior indicates that the polarization of the samples obeys the Debye model [31]. Here, again we have found that the temperature dependence of dielectric relaxation peak  $\omega_m$  obeys Arrhenius formula (Table 2).

**Fig. 5** Variation of conductivity with frequency at various temperature for PIn with stoichiometric ratios of indole and  $\text{FeCl}_3$  as (a) 70:30, (b) 60:40, (c) 50:50, (d) 40:60 and (e) 30:70 Wt %



**Fig. 6** Frequency dependence plot of real part of dielectric constant for PIn with (40:60) wt% of indole and  $\text{FeCl}_3$



**Fig. 7** Frequency dependence plot of imaginary part of dielectric constant for PIn with (40:60) wt% of indole and  $\text{FeCl}_3$



### 3.5. Modulus analysis

An alternative approach to investigate the complex electrical response of materials is referred as electric modulus, which compensates the electrode polarization effect. The complex electric modulus ( $M^*$ ) is the reciprocal of the complex permittivity ( $\epsilon^*$ ).

$$M^* = \frac{1}{\epsilon^*} \quad (3)$$

$$M^* = M' + jM'' \quad (4)$$

where  $M'$  real and  $M''$  imaginary parts of complex electric modulus. The real and imaginary parts of the modulus data are calculated using the impedance data of glasses measured at different temperatures using the following equations.

$$M' = \frac{\omega A \epsilon_0 Z''}{t} \quad (5)$$

$$M'' = \frac{\omega A \epsilon_0 Z'}{t} \quad (6)$$

where  $\omega$  is the angular frequency,  $\epsilon_0$  the permittivity of free space,  $A$  the area of cross section and  $t$  thickness of the material [36, 37].

Figure 8 shows the  $M'$  versus  $\log(\omega)$  for PIn with (40:60) wt% of indole and  $\text{FeCl}_3$  at different temperatures. In the modulus curves, the continuous line represents guide to eye of  $M'$  curve, whereas the symbols correspond to the experimental data. At higher frequencies,  $M'$  reaches a maximum constant value  $M_\infty = 1/\epsilon_\infty$  and at low frequencies  $M'$  approaches to zero indicates that the electrode polarization makes a negligible contribution. The dispersion in between these frequencies is due to the conductivity relaxation.

Figure 9 represents the  $M''$  versus  $\log(\omega)$  spectra plotted at different temperatures for PIn with (40:60) wt% of indole and  $\text{FeCl}_3$ . It is observed that the shape of each curve is asymmetric of non-Lorentzian type and with temperature, the position of the peak frequency shifted towards the higher frequency region. It could be explained based on the distribution of attempt frequencies for the barrier crossover or a distribution of jump or flight distances following the crossover [36, 38].

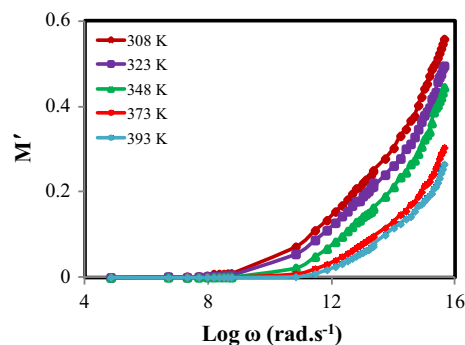


**Fig. 8** Real part of the modulus versus  $\log(\omega)$  for PIn with (40:60) wt% of indole and  $\text{FeCl}_3$

Two apparent relaxation regions appear in the plot of  $M''$  versus  $\log(\omega)$ , the region towards the left of the peak (below 800 kHz) is associated to the conduction process where the charge carriers are mobile over a long distance. The region towards the right of the peak (above 800 kHz) is associated with the relaxation polarization process where the charge carriers are spatially confined to the potential wells [36]. Similar behaviour is also observed in case of the other samples. The non-symmetric modulus plot has been expressed by stretching exponential relaxation (decay) function.

The dissipation factor  $\tan(\delta) = \epsilon''/\epsilon'$  reflects the phase difference due to the loss of energy within the sample at a particular frequency. The frequency dependence of  $\tan(\delta)$  at different temperatures for PIn with (40:60) wt% of indole and  $\text{FeCl}_3$  is shown in Fig. 10. At lower frequency region  $\tan(\delta)$  increases with rise in frequency and shows a maximum at particular frequencies for different temperatures. These maxima of frequency shifted towards an increase in frequency for the rise in temperatures. The increase in  $\tan(\delta)$  may be due to the active component than its reactive component. At higher frequency region,  $\tan(\delta)$  is decreases with frequency due to the increased reactive component, whereas the active component of the current is practically independent of frequency [38]. The observed dielectric loss may be due to two main contributions. A first part is the thermally activated relaxation of the Debye-type freely rotating dipoles in which the thermal energy is

**Table 2** Values of dielectric constants  $\epsilon'$  and  $\epsilon''$  (at 20 Hz and 1 MHz) for temperature 393 K of as-synthesized PIn with different stoichiometric ratio of indole and  $\text{FeCl}_3$

wt% ratios	$\epsilon'$ (at 20 Hz)	$\epsilon'$ (at 1 MHz)	$\epsilon''$ (at 20 Hz)	$\epsilon''$ (at 1 MHz)
70:30	8361.66	1.76	193.16	1.54
60:40	11,232.64	0.52	378.76	0.54
50:50	10,854.46	0.41	165.86	0.84
40:60	8654.98	0.29	112.76	0.87
30:70	7858.65	0.42	109.65	0.72

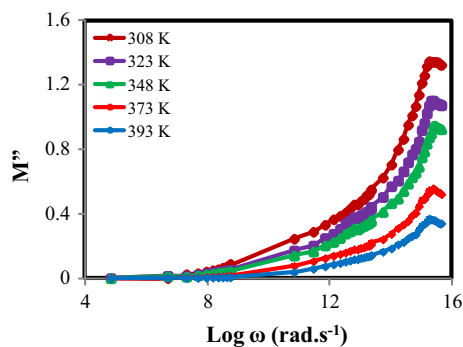


**Fig. 9** Imaginary part of the modulus versus  $\log(\omega)$  for PIn with (40:60) wt% of indole and  $\text{FeCl}_3$

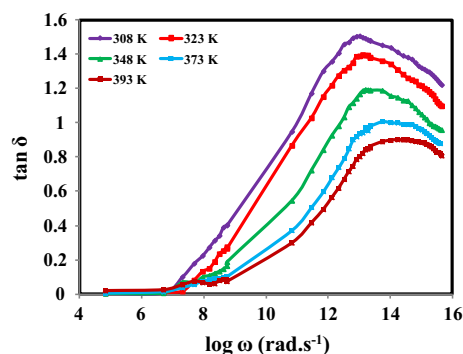


**Fig. 10** Variation of  $\tan(\delta)$  versus  $\log(\omega)$  for PIn with (40:60) wt% of indole and  $\text{FeCl}_3$  for different temperature

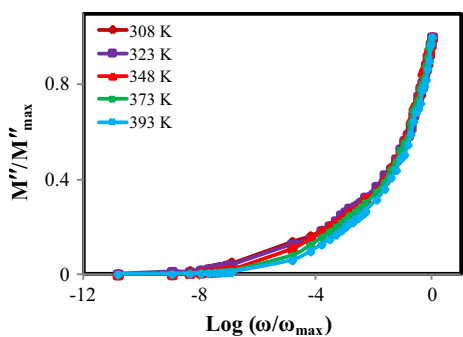


**Fig. 11** Variation of  $M''/M''_{\max}$  with  $\text{Log}(\omega/\omega_{\max})$  for PIn with (40:60) wt% of indole and  $\text{FeCl}_3$  at different temperatures

the only type of excitation. A second part occurs at higher temperatures, which increases with temperature and is due to electrical condition in which there is an electron phonon interaction [39].

$M''/M''_{\max}$  versus  $\text{Log}(\omega/\omega_{\max})$  plots for PIn with (40:60) wt% of indole and  $\text{FeCl}_3$  at different temperatures are shown in Fig. 11. From figure, it is clear that, the relaxation mechanism is temperature independent since all the curves merged into a single master curve. This phenomenon of relaxation mechanism is also reported [40].

#### 4. Conclusions

In summary, we have investigated the electrical behavior of chemically synthesized conducting PIn. The principal bonding present in as-synthesized PIn powder samples was confirmed from FTIR spectroscopy, whereas XRD profile reflected the amorphous nature. The thermal study ensured that, the as-synthesized samples have fairly good thermal stability. The frequency dependence of AC conductivity follows the universal power law. Dielectric behaviors of these samples reveal the situation that the conducting PIn exhibit a decrease in dielectric constant and dielectric loss with frequency and temperature. The decrease in dielectric constant with frequency is attributed to polar nature of the material. The modulus analysis study reveals that the electrode polarization has negligible contribution and conjointly shows non-Debye nature of as-synthesized samples. The  $\tan(\delta)$  peak shifts to a higher frequency with increasing temperature and is positioned at low frequency region. The results have also showed the potential of as-synthesized samples for energy storage application in electronics devices such supercapacitor and rechargeable battery applications.

**Acknowledgements** Authors are very much thankful to Head, Department of Physics Sant Gadge Baba Amravati University, Amravati for providing the necessary facilities.

#### Compliance with ethical standards

**Conflict of interest** The authors declare that they have no conflict of interest.

#### References

- [1] P C Pandey and R Prakash *J. Electrochem. Soc.* **145** 999 (1998)
- [2] F F Fusalba and D Belanger *J. Phys. Chem. B* **103** 9033 (1999)
- [3] P C Pandey, D S Chauhan and V Singh *Mat. Sci. Eng. C* **32** 1 (2012)
- [4] V Singh, S Mohan, G Singh, P C Pandey and R Prakash *Sens. Actuator B Chem.* **132** 99 (2008)
- [5] B Gupta and R Prakash *Mat. Sci. Eng. C* **29** 1746 (2009)
- [6] P Burgmayer and R W Murray *J. Electroanal. Chem.* **147** 339 (1983)
- [7] O Inganas and I Lundstrom *J. Electrochem. Soc.* **131** 1129 (1984)
- [8] J Xu, W Zhou, J Hou, S Pu, L Yan and J Wang *Mat. Lett.* **59** 2412 (2005)
- [9] S P Koiry, V Saxena, D Sutar, S Bhattacharya, D K Aswal, S K Gupta and J V Yakhmi *J. Appl. Polym. Sci.* **103** 595 (2007)
- [10] H Talbi and D Billaud *Synth. Met.* **98** 105 (1998)
- [11] D Billaud and E B Hannecart *Synth. Met.* **69** 571 (1995)
- [12] M Yurtsever and E Yurtsever *Polym.* **43** 6019 (2002)
- [13] L Joshi and R Prakash *Mat. Lett.* **65** 3016 (2011)
- [14] M Laridjani, J P Pouget, E M Scherr, A G MacDiarmid, M E Jozefowicz and A J Epstein *Macromol.* **25** 4106 (1992)
- [15] A T Bieganski, A Michota, J Bukowska and K Jackowska *Bioelectrochem.* **69** 41 (2006)



- [16] P J Kinlen, J Liu, Y Ding, C R Graham and E E Remsen *Macromol.* **31** 1735 (1998)
- [17] G Rajasudha, H Shankar, P Thangadurai, N Boukos, V Narayanan and A Stephen *Ionics* **16** 839 (2010)
- [18] N S Wadatkar and S A Waghuley *Egypt. J. Basic Appl. Sci.* **2** 19 (2015)
- [19] D S Kelkar and A B Chourasia *Indian J. Phys.* **86** 101 (2012)
- [20] Y Ding, A B Padias and H K Hall *J. Polym. Sci. Part A Polym. Chem.* **37** 2569 (1999)
- [21] A Kumar, A C Pandey and R Prakash *Catal. Sci. Technol.* **2** 2533 (2012)
- [22] P S Abthagir, K Dhanalakshmi and R Saraswathi *Synth. Met.* **93** 1 (1998)
- [23] R Lazzaroni, A De Pryck, C H Debraisieux, J Riga, J Verbist, J L Bredas, J Delhalle and J M Andre *Synth. Met.* **21** 189 (1987)
- [24] H I Unal, B Sahan and O Erol *Mat. Chem. Phys.* **134** 382 (2012)
- [25] S A Waghuley, S M Yenorkar, S S Yawale and S P Yawale *Sens. Actuators B Chem.* **128** 366 (2008)
- [26] P S Abthagir and R Saraswathi *Thermochim. Acta* **424** 25 (2004)
- [27] S A Waghuley *J. Pure Appl. Phys.* **49** 816 (2011)
- [28] M T Raman, M Vargas and C V Raman *J. Alloys Comp.* **617** 547 (2014)
- [29] A Dutta, T P Sinha, P Jena and S Adak *J. Non Cryst. Solids* **354** 3952 (2008)
- [30] C R Mariappan, G Govindara, S VinothRathan and G Vijaya-Prakash *Mat. Sci. Eng. B* **121** 2 (2005)
- [31] M H Makled, E Sheha, T S Shanap and M K El-Mansy *J. Adv. Res.* **4** 531 (2013)
- [32] B H Rudramadevi, K Thilagavathi and S Buddhudu *Indian J. Phys.* **86** 997 (2012)
- [33] P K C Pillal and Rashmi *Int. J. Polym. Mat.* **8** 255 (1980)
- [34] Y Fu, K Pathmanathan and J R Stevens *J. Chem. Phys.* **94** 6323 (1991)
- [35] P Dutta, S Biswas and S K De *Mat. Res. Bull.* **37** 193 (2002)
- [36] S Kulkarni, B M Nagabhushana, N Parvatikar, A Koppalkar, C Shivakumara and R Damle *Mat. Res. Bull.* **50** 197 (2014)
- [37] D K Pradhan, R P N Choudhary and B K Samantaray *Int. J. Electrochem. Sci.* **3** 597 (2008)
- [38] R Baskaran, S Selvasekarapandian, G Hirankumar and M S Bhuvaneshwari *J. Power Sources* **134** 235 (2004)
- [39] E E Shaishay, S F El-Desouki, I Shaltout and A A Bahgat *J. Mat. Sci. Technol.* **22** 701 (2006)
- [40] R Cheruku, L Vijayan and G Govindaraj *Mat. Sci. Eng. B* **177** 771 (2012)